# Spin transport in graphene - hexagonal boron nitride van der Waals heterostructures

Gurram, Mallikarjuna



*Publication date:*
2018

# Appendix A

# Appendix: Theory


**Abstract**

*In this Appendix, a derivation of the nonlocal resistance $R_{nl}$ is given by considering a one dimensional spin diffusion transport in a non-magnetic channel. At first, a relation between the nonlocal voltage $V$ and the spin chemical potential underneath the detector $\mu_s^N(x = L)$ is derived. Then the Bloch equation is solved for the spin diffusion in the non-magnetic channel to find $\mu_s^N(x = L)$. The derivations given here follow the analysis from Refs.[1–4]. A special case of three-terminal geometry is also considered for deriving the expression for the Hanle spin precession signal.*


## A.1 Nonlocal spin transport

### A.1.1 Spin injection: Nonlocal

**Injection Ferromagnet(at x=0):** In a typical lateral non-local spin valve measurements, F lies across the width of the N. Consider the geometry and directions depicted in the schematics of a non-local spin injection and detection technique (Fig. 2.2). The charge current $I^{\mathrm{F}}$, and the spin current $I_{\mathrm{s}}^{\mathrm{F}}$ associated with it being injected along $-\hat{z}$, where $j^{\mathrm{F}} = I^{\mathrm{F}}/(W^{\mathrm{N}}W^{\mathrm{F}})$ and $j_{\mathrm{s}}^{\mathrm{F}} = I_{\mathrm{s}}^{\mathrm{F}}/(W^{\mathrm{N}}W^{\mathrm{F}})$ with the width of the non-magnet ($W^{\mathrm{N}}$), and the ferromagnet ($W^{\mathrm{F}}$).

For the injector F/N contact at x=0, we can do the similar analysis as in section 2.2 to obtain the spin accumulation in F1 $\mu_{\mathrm{s}}^{\mathrm{F1}}(z)$, the spin current density in F1 $j_{\mathrm{s}}^{\mathrm{F1}}$, and the spin current across the F/N contact $j_{\mathrm{s}}^{\mathrm{C1}}$. We can also obtains the spin injection efficiency or the current spin polarization of the injection contact $P_{\mathrm{in}} = \frac{j_{\mathrm{s}}}{j}$, given by:

$$P_{\mathrm{in}}^{\mathrm{C1}} = \frac{P_{\sigma}^{\mathrm{F1}} R^{\mathrm{F1}} + P_{\sigma}^{\mathrm{C1}} R^{\mathrm{C1}}}{R^{\mathrm{F1}} + R^{\mathrm{C1}} + R^{\mathrm{N}}} \tag{A.1}$$

where, superscripts $F1$ ($F2$) and $C1$ ($C2$) represents the F and C at the injector, x=0(detector, x=L). where $R^{\mathrm{F}}$ is the effective resistance of F,

$$R^{\mathrm{F}} = \frac{\lambda^{\mathrm{F}}}{W^{\mathrm{N}}W^{\mathrm{F}}\sigma^{\mathrm{F}}} \frac{R_{\mathrm{s}}^{\mathrm{F}}}{(1 - {P_{\sigma}^{\mathrm{F}}}^2)}, \tag{A.2}$$

$R^{\mathrm{C1}}$ is the effective resistance of the injector F/N contact,

$$R^{\mathrm{C1}} = \frac{1}{W^{\mathrm{N}} W^{\mathrm{F}} \sigma^{\mathrm{C1}}} \frac{R_{\mathrm{s}}^{\mathrm{C1}}}{(1 - P_{\sigma}^{\mathrm{C1}^2})}, \tag{A.3}$$

$R^{\mathrm{N}}$ is the effective resistance or spin resistance ($R_{\mathrm{s}}^{\mathrm{N}}$) of the N,

$$R^{\mathrm{N}} = R_{\mathrm{s}}^{\mathrm{N}} = \frac{\lambda^{\mathrm{N}}}{W^{\mathrm{N}} \sigma^{\mathrm{N}}}. \tag{A.4}$$

### A.1.2 Spin detection: Nonlocal

In the non-local measurement geometry, the electrical spin is injected from F at x=0 (F1). The injected spin accumulation diffuses along either side of F1 along $\hat{x}$ and detected by another F at x=L (F2) by the Johnson-Silsbee spin-charge coupling[5, 6]. Since the injected charge current $I$ flows along -$\hat{x}$, there is no charge current flow at the detector at x=+L. When a high resistance probe (voltmeter) is connected across the detector F2 and far end of N, an electro motive force (emf) appears in the circuit which is the difference in chemical potentials at the both ends. The emf can be detected as (non-local)voltage drop ($V$) across the F/N detector contact, given by

$$V = \mu^{\mathrm{N}}(x = \infty, z = 0) - \mu^{\mathrm{FL}}(x = L, z = \infty) \tag{A.5}$$

**Detection Ferromagnet(at x=L):** For the F/N detector at x=L, $I = 0$. By assuming a finite $\mu_{\mathrm{s}}^{\mathrm{FL}}(z = \infty)$, one can integrate Eq. 2.6 for F2 at x=L,

$$\mu^{\mathrm{F2}}(z = \infty) - \mu^{\mathrm{F2}}(z = 0) = P_{\sigma}^{\mathrm{F2}} \mu_{\mathrm{s}}^{\mathrm{F2}}(z = 0) \tag{A.6}$$

and for N at z=0,

$$\mu^{\mathrm{N}}(x = \infty) = \mu^{\mathrm{N}}(x = L) \tag{A.7}$$

**Detection F/N contact(at x=L):** The chemical potential difference for the F/N contact at x=L is given by,

$$\mu^{\mathrm{N}}(z = 0) - \mu^{\mathrm{F2}}(z = 0) = -P_{\sigma}^{\mathrm{C2}}[\mu_{\mathrm{s}}^{\mathrm{N}}(z = 0) - \mu_{\mathrm{s}}^{\mathrm{F}}(z = 0)] \tag{A.8}$$

Therefore, $V$ from Eq. A.5 can be written as,

$$V = (-P_{\sigma}^{\mathrm{C2}}[\mu_{\mathrm{s}}^{\mathrm{N}}(z = 0) - \mu_{\mathrm{s}}^{\mathrm{F}}(z = 0)] - P_{\sigma}^{\mathrm{F2}}[\mu_{\mathrm{s}}^{\mathrm{F2}}(z = 0)] \tag{A.9}$$

The spin current in the detector ferromagnet F2 and the detector F/N contact C2 can be written (similar to that of for F1 Eq. 2.12 and C1 Eq. 2.14),

$$\begin{aligned} j_{\mathrm{s}}^{\mathrm{F2}}(z) &= -\frac{\mu_{\mathrm{s}}^{\mathrm{F2}}(z)}{R^{\mathrm{F2}}} \\ j_{\mathrm{s}}^{\mathrm{C2}} &= \frac{[\mu_{\mathrm{s}}^{\mathrm{F2}}(0) - \mu_{\mathrm{s}}^{\mathrm{N2}}(0)]}{R^{\mathrm{C2}}} \end{aligned} \tag{A.10}$$

Assuming the continuity of the spin current for the detector contact:

$$j_s^{F2} = j_s^{C2}(z = 0) \tag{A.11}$$

From Eqs. A.10 and A.11, the spin current in the detector is obtained:

$$\begin{aligned} j_s^{C2}(z = 0)(R^{F2} + R^{C2}) &= -\mu_s^N(z = 0) \\ \mu_s^{F2} &= \frac{R^{F2}\mu_s^N}{R^{F2} + R^{C2}} \end{aligned} \tag{A.12}$$

Using Eqs. A.12 and A.9, the voltage across the detector contact is obtained,

$$V = -\frac{P_\sigma^{F2}R^{F2} + P_\sigma^{C2}R^{C2}}{R^{F2} + R^{C2}}\mu_s^N(x = L) \tag{A.13}$$

Here, the value of spin accumulation beneath the detector contact $\mu_s^N(x = L)$ can be obtained by solving the diffusion equation for the N, as described in the next section.

The *spin detection polarization* ($P_d^{C2}$) of the F/N detector contact is defined as the ratio of the voltage being measured to the spin accumulation underneath the detector contact,

$$P_d^{C2} = \frac{V}{\mu_s^N(x = L)} = \frac{P_\sigma^{F2}R^{F2} + P_\sigma^{C2}R^{C2}}{R^{F2} + R^{C2}} \equiv P_{in}^{C2}\frac{R^{F2} + R^{C2} + R^N}{R^{F2} + R^{C2}} \tag{A.14}$$

Note that *spin detection polarization* $P_d^{C2}$ cannot be defined in the form of a ratio of spin current to the charge current, and its form is different from the *current spin injection polarization* that is defined earlier for the *injector contact* $P_{in}^{C1}$ (Eq. A.1). Moreover, under the condition of the large contact resistance for the detector, i.e., $R^{C2} \gg (R^{F2}, R^N)$, the spin detection polarization becomes equivalent to its current spin injection polarization and , $P_d^{C2} \simeq P_{in}^{C2}$. Therefore, for high resistance contacts, we can use the spin injection and detection polarization anonymously. However, under the application of external bias across a contact, its spin injection and detection polarization are different (see Chapter 6).

When the non-equilibrium spin accumulation is finite at the far end of the N, i.e, $\mu_s^N(x \longrightarrow \infty) \neq 0$, above equation can also be written as[7],

$$V = -\frac{P_\sigma^{F2}R^{F2} + P_\sigma^{C2}R^{C2}}{R^{F2} + R^{C2} + R^N}\mu_s^N(x = \infty) \equiv -P_d^{C2}\mu_s^N(x = \infty) \tag{A.15}$$

A

### A.1.3 Spin diffusion: Nonlocal

**Non-magnetic diffusion channel:** The transport of spins in N can be described by considering two spin current channels for up-spin and down-spin[8], using the spin diffusion equation in the steady state 2.10.

To obtain $\mu_{\mathrm{s}}^{\mathrm{N}}(x = L)$ in Eq. A.13, consider a general case where the spins also precess in the presence of external magnetic field applied normal to the spin injection in N, i.e, **B** = $B_z\hat{z}$. In case of spin precession during the spin transport in N, one needs to solve the Bloch equation for $\mu_{\mathrm{s}}^{\mathrm{N}}(x = L)$:

$$\frac{d\mu_{\mathrm{s}}^{\mathrm{N}}}{dt} = D_{\mathrm{s}} \bigtriangledown^2 \mu_{\mathrm{s}}^{\mathrm{N}} - \frac{\mu_{\mathrm{s}}^{\mathrm{N}}}{\tau} + \omega_L \times \mu_{\mathrm{s}}^{\mathrm{N}} \tag{A.16}$$

where $\mu_{\mathrm{s}}$ is the spin accumulation in 3D, $D_{\mathrm{s}}$ is the spin diffusion constant, $\tau_{\mathrm{s}}$ is the spin relaxation time, and $\omega_L = \frac{g\mu_B B_z}{\hbar}$ is the Larmor precession frequency caused by the magnetic field $B_z$, Bohr magneton $\mu_B$, and the gyromagnetic factor g(=2 for electrons). The spin current in the non-local channel of N where the charge current is zero, is given by(using Eq. 2.13),

$$I_{\mathrm{s}}^{\mathrm{N}} = -W^{\mathrm{N}}\sigma^{\mathrm{N}} \bigtriangledown \mu_{\mathrm{s}}^{\mathrm{N}} = -\lambda^{\mathrm{N}} \frac{\bigtriangledown \mu_{\mathrm{s}}^{\mathrm{N}}}{R^{\mathrm{N}}} \tag{A.17}$$

where $R^{\mathrm{N}}(= R_{\mathrm{s}}^{\mathrm{N}})$ is the effective resistance or spin resistance of the N, given by Eq. A.4.

The above equations describe the diffusion of spin accumulation $\mu_{\mathrm{s}}^{\mathrm{N}} = \mu_{\mathrm{sx}}^{\mathrm{N}}\hat{x} + \mu_{\mathrm{sy}}^{\mathrm{N}}\hat{y} + \mu_{\mathrm{sz}}^{\mathrm{N}}\hat{z}$ in 3D. However, in the case of very thin N materials like graphene, spin diffusion in the direction normal to the surface can be ignored, limiting the diffusion to 2D. When the spin injection contacts laid across the width of the 2D N and the spin injection is assumed to be uniform across the F/N interface, the spin diffusion can be further reduced to 1D.

Consider the 1D spin diffusion in the N, say, along x-direction, then the above equation can be written in the steady state ($\frac{d\mu_{\mathrm{s}}^{\mathrm{N}}}{dt}$=0) as,

A

$$D\frac{d^2}{dx^2}\begin{pmatrix}\mu_{\mathrm{sx}}^{\mathrm{N}}\\ \mu_{\mathrm{sy}}^{\mathrm{N}}\end{pmatrix} - \frac{1}{\tau_{\mathrm{s}}}\begin{pmatrix}\mu_{\mathrm{sx}}^{\mathrm{N}}\\ \mu_{\mathrm{sy}}^{\mathrm{N}}\end{pmatrix} + \omega_L\begin{pmatrix}-\mu_{\mathrm{sy}}^{\mathrm{N}}\\ \mu_{\mathrm{sx}}^{\mathrm{N}}\end{pmatrix} = 0 \tag{A.18a}$$

$$D\frac{d^2\mu_{\mathrm{sz}}^{\mathrm{N}}}{dx^2} - \frac{\mu_{\mathrm{sz}}^{\mathrm{N}}}{\tau_{\mathrm{s}}} = 0 \tag{A.18b}$$

Then the solution to the above equations under the boundary conditions $\mu_{sx,sy,sz}^{\mathrm{N}}(x \longrightarrow$

$\pm\infty) \longrightarrow 0$, is given by,

$$\mu^{\text{N}}_{\text{sz}} = \begin{cases} \mu^{\text{N-}}_{\text{sz}} = A^{+}e^{+k_1 x}, & x \leq 0 \\ \mu^{\text{N0}}_{\text{sz}} = A^{+}_{0}e^{+k_1 x} + A^{-}_{0}e^{-k_1 x}, 0 < x < L \\ \mu^{\text{N+}}_{\text{sz}} = A^{-}e^{-k_1 x}, & x \geq 0 \end{cases} \tag{A.19}$$

$$\mu^{\text{N}}_{\text{sx}} = \begin{cases} \mu^{\text{N-}}_{\text{sx}} = B^{+}e^{+k_2 x} + C^{+}e^{+\widetilde{k_2} x}, & x \leq 0 \\ \mu^{\text{N0}}_{\text{sx}} = B^{+}_{0}e^{+k_2 x} + B^{-}_{0}e^{-k_2 x} + C^{+}_{0}e^{+\widetilde{k_2} x} + C^{-}_{0}e^{-\widetilde{k_2} x}, 0 < x < L \\ \mu^{\text{N+}}_{\text{sx}} = B^{-}e^{+k_2 x} + C^{-}e^{+\widetilde{k_2} x}, & x \geq 0 \end{cases} \tag{A.20}$$

$$\mu^{\text{N}}_{\text{sy}} = \begin{cases} \mu^{\text{N-}}_{\text{sy}} = -iB^{+}e^{+k_2 x} + iC^{+}e^{+\widetilde{k_2} x}, & x \leq 0 \\ \mu^{\text{N0}}_{\text{sy}} = -iB^{+}_{0}e^{+k_2 x} - iB^{-}_{0}e^{-k_2 x} + iC^{+}_{0}e^{+\widetilde{k_2} x} + iC^{-}_{0}e^{-\widetilde{k_2} x}, 0 < x < L \\ \mu^{\text{N+}}_{\text{sy}} = -iB^{-}e^{+k_2 x} + iC^{-}e^{+\widetilde{k_2} x}, & x \geq 0 \end{cases} \tag{A.21}$$

where $k_1 = \frac{1}{\lambda}$, $k_2 = k_1 \frac{1}{1+i\omega\tau}$, and $\widetilde{k_2}$ is the complex conjugate of $k_2$. The constants in the above equations can be determined by imposing the boundary conditions. The equations with boundary condition on continuity of $\mu^{\text{N}}_{\text{s}}$ at x=0 and x=L can be written as,

$$\text{at x=0} \quad \begin{cases} \mu^{\text{N-}}_{\text{sz}}(x=0) = \mu^{\text{N0}}_{\text{sz}}(x=0) \\ \mu^{\text{N-}}_{\text{sx}}(x=0) = \mu^{\text{N0}}_{\text{sx}}(x=0) \\ \mu^{\text{N-}}_{\text{sy}}(x=0) = \mu^{\text{N0}}_{\text{sy}}(x=0) \end{cases} \tag{A.22}$$

$$\text{at x=L} \quad \begin{cases} \mu^{\text{N-}}_{\text{sz}}(x=L) = \mu^{\text{N0}}_{\text{sz}}(x=L) \\ \mu^{\text{N-}}_{\text{sx}}(x=L) = \mu^{\text{N0}}_{\text{sx}}(x=L) \\ \mu^{\text{N-}}_{\text{sy}}(x=L) = \mu^{\text{N0}}_{\text{sy}}(x=L) \end{cases} \tag{A.23}$$

Another boundary condition on conservation of spin current at each contact gives,

$$\text{At x=0 :} \quad I^{\text{C}}_{\text{s}}(x=0)(-\hat{z}) = I^{\text{N-}}_{\text{sx}}(x=0)(-\hat{x}) + I^{\text{N0}}_{\text{sx}}(x=0)(\hat{x}) \tag{A.24}$$

$$\Longrightarrow \begin{cases} -\bigtriangledown\mu^{\text{N-}}_{\text{sz}}(x=0) + \bigtriangledown\mu^{\text{N0}}_{\text{sz}}(x=0) - \frac{1}{r_0}\mu^{\text{N}}_{\text{sz}}(x=0) = 0 \\ -\bigtriangledown\mu^{\text{N-}}_{\text{sx}}(x=0) + \bigtriangledown\mu^{\text{N0}}_{\text{sx}}(x=0) - \frac{1}{r_0}\mu^{\text{N}}_{\text{sx}}(x=0) = \Delta \\ -\bigtriangledown\mu^{\text{N-}}_{\text{sy}}(x=0) + \bigtriangledown\mu^{\text{N0}}_{\text{sy}}(x=0) - \frac{1}{r_0}\mu^{\text{N}}_{\text{sy}}(x=0) = 0 \end{cases} \tag{A.25}$$

$$\text{And, at x=L :} \quad I^{\text{C}}_{\text{s}}(x=L)(-\hat{z}) = I^{\text{N0}}_{\text{sx}}(x=L)(-\hat{x}) + I^{\text{N+}}_{\text{sx}}(x=L)(\hat{x}) \tag{A.26}$$

$$\Longrightarrow \begin{cases} -\bigtriangledown\mu^{\text{N0}}_{\text{sz}}(x=L) + \bigtriangledown\mu^{\text{N+}}_{\text{sz}}(x=L) - \frac{1}{r_L}\mu^{\text{N}}_{\text{sz}}(x=L) = 0 \\ -\bigtriangledown\mu^{\text{N0}}_{\text{sx}}(x=L) + \bigtriangledown\mu^{\text{N+}}_{\text{sx}}(x=L) - \frac{1}{r_L}\mu^{\text{N}}_{\text{sx}}(x=L) = 0 \\ -\bigtriangledown\mu^{\text{N0}}_{\text{sy}}(x=L) + \bigtriangledown\mu^{\text{N+}}_{\text{sy}}(x=L) - \frac{1}{r_L}\mu^{\text{N}}_{\text{sy}}(x=L) = 0 \end{cases} \tag{A.27}$$

where the r-parameter[2], $r = W^{\mathrm{N}}\sigma^{\mathrm{N}}(R^{\mathrm{F}} + F^{\mathrm{C}})$, defined for the injector ($r_1$) and the detector($r_2$) F/N contacts, and

$$
\begin{aligned}
r &= W^{\mathrm{N}}\sigma^{\mathrm{N}}(R^{\mathrm{F}} + R^{\mathrm{C}}) \\
\Delta &= \frac{I}{W^{\mathrm{N}}\sigma^{\mathrm{N}}}\frac{P_\sigma^{\mathrm{F1}}R^{\mathrm{F1}} + P_\sigma^{\mathrm{C1}}R^{\mathrm{C1}}}{R^{\mathrm{F1}} + R^{\mathrm{C1}}} \equiv \frac{I}{W^{\mathrm{N}}\sigma^{\mathrm{N}}}P_{\mathrm{in}}^{\mathrm{C1}} = IP_{\mathrm{d}}^{\mathrm{C1}}\frac{R_1}{r_1}
\end{aligned}
\tag{A.28}
$$

$$
P_{\mathrm{d}}^{\mathrm{C1}} = \frac{P_\sigma^{\mathrm{F1}}R^{\mathrm{F1}} + P_\sigma^{\mathrm{C1}}R^{\mathrm{C1}}}{R^{\mathrm{F1}} + R^{\mathrm{C1}}}
$$

where $P_{\mathrm{d}}^{\mathrm{C1}}$ is the *spin detection polarization* of the injector contact C1 at x=0, similar to *spin detection polarization* of the detector contact C2 $P_{\mathrm{d}}^{\mathrm{C2}}$ in Eq. A.14 in the four-terminal nonlocal measurement geometry[Fig. 2.2].

The above system of equations can be solved, for example, using MATLAB program, to obtain the 12 constants. Therefore the value of interest, $\mu_{\mathrm{sy}}^{\mathrm{N}}(x = L) = -iB^-e^{+k_2x} + iC^-e^{+\widetilde{k_2x}}$, is determined as

$$
\mu_{\mathrm{sy}}^{\mathrm{N}}(x = L) = -2\Re\left\{\frac{\Delta r_1 r_2 k_2 e^{-k_2L}}{(1 + 2r_1k_2)(1 + 2r_2k_2) - e^{-2k_2L}}\right\} \tag{A.29}
$$

where $\Re$ denotes the real part.

Using Eq. A.28, the $V$ from Eq. A.13 can be written as,

$$
V = -P_{\mathrm{d}}^{\mathrm{C2}}\frac{R_2}{r_2}\frac{\lambda^{\mathrm{N}}}{R^{\mathrm{N}}}\mu_{\mathrm{s}}^{\mathrm{N}}(x = L) \tag{A.30}
$$

Combining Eqs. A.29 and A.30, the non-local resistance $R_{\mathrm{nl}} = \frac{V}{I}$ in the presence of the external magnetic field and thus the spin precession is given by,

$$
R_{\mathrm{nl}} = \pm\frac{1}{2}P_{\mathrm{in}}^{\mathrm{C1}}P_{\mathrm{d}}^{\mathrm{C2}}R^{\mathrm{N}}\Re\left\{\lambda^{\mathrm{N}}k_2\frac{4e^{-k_2L}}{(1 + 2r_1k_2)(1 + 2r_2k_2) - e^{-2k_2L}}\right\}\left[\frac{R_1R_2}{R^{\mathrm{N}2}}\right] \tag{A.31}
$$

## A.2 Three-terminal Hanle measurements

For a long time, spin polarization in semiconductors (SC) was studied either by optical injection and optical detection[9, 10], or by electrical injection and optical detection[7, 11, 12] techniques. Both methods have been widely used for GaAs due to its direct bandgap. However, due to indirect bandgap in Si, the efficiency of the creation and detection of spin polarization in Si is limited[13].

On the other hand, all-electric spin injection and detection in the non-local lateral geometry for the semiconductors was challenging due to the conductivity mismatch problem. Therefore, a three-terminal (3T) Hanle measurement technique was developed to demonstrate the electrical injection and detection of spin accumulation in a

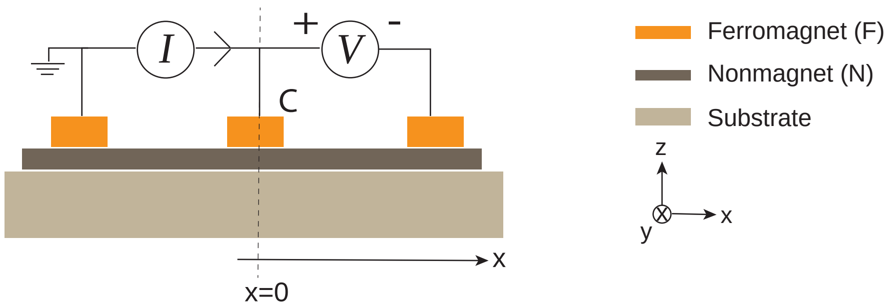


**Figure A.1:** Three-terminal Hanle spin precession measurement geometry. Only one F/N contact is used for both the electrical spin injection and detection.

semiconductor, first at low temperature by Lou *et al*.[14](n-GaAs, below 60 K), and later at room temperature by Dash *et al*.[15](n-Si and p-Si).

In a three-terminal Hanle geometry (Fig. A.1), a single magnetic tunnel contact is used for electrical injection and detection of the non-equilibrium spin accumulation underneath the contact. The measurement geometry is equivalant to the 4T non-local Hanle measurement geometry with L=0. The measured signal includes the charge contribution part which is due to the contact resistance ($R^{\mathrm{C}}$) and the spin contribution part which is due to the spin accumulation under the contact.

The spin parameters of N can be characterized from the three-terminal Hanle measurements where, similar to a four-terminal nonlocal Hanle measurement, a magnetic field is applied perpendicular to the plane of the spin injection. The field depolarizes the injected spin accumulation due to the spin precession, and the resulting signal due to the Hanle effect for the tunneling contact($P_{\mathrm{in}}^{\mathrm{C}} \sim P_{\mathrm{d}}^{\mathrm{C}} \equiv P^{\mathrm{C}}$) can be written as:

$$R_{3T}(B) = R^{\mathrm{C}} + \frac{1}{2} {P^{\mathrm{C}}}^2 R^{\mathrm{N}} \Re \left\{ \frac{1}{\sqrt{1 + j\omega\tau}} \right\} \tag{A.32}$$

## *References*


[1] Jedema, F. Electrical spin injection in metallic mesoscopic spin valves (2002). Relation: http://www.rug.nl/ date˙submitted:2003 Rights: University of Groningen.

[2] Popinciuc, M. *et al.* Electronic spin transport in graphene field-effect transistors. *Phys. Rev. B* **80**, 214427 (2009).

[3] Takahashi, S. & Maekawa, S. Spin injection and detection in magnetic nanostructures. *Phys. Rev. B* **67**, 052409 (2003).

[4] Sosenko, E., Wei, H. & Aji, V. Effect of contacts on spin lifetime measurements in graphene. *Phys. Rev. B* **89**, 245436 (2014).

[5] Silsbee, R. H. Novel method for the study of spin tranport in conductors. *Bull. Magn. Reson.* **2**, 284–285 (1980).

[6] Johnson, M. & Silsbee, R. H. Spin-injection experiment. *Phys. Rev. B* **37**, 5326–5335 (1988).

[7] Fabian, J. *et al.* Semiconductor spintronics. *Acta Physica Slovaca* **57**, 565 907 (2007).

[8] Valet, T. & Fert, A. Theory of the perpendicular magnetoresistance in magnetic multilayers. *Phys. Rev. B* **48**, 7099–7113 (1993).

[9] Fishman, G. & Lampel, G. Spin relaxation of photoelectrons in p-type gallium arsenide. *Phys. Rev. B* **16**, 820 (1977).

[10] Kikkawa, J. & Awschalom, D. All-optical magnetic resonance in semiconductors. *Science* **287**, 473–476 (2000).

[11] Ohno, Y. *et al.* Electrical spin injection in a ferromagnetic semiconductor heterostructure. *Nature* **402**, 790 (1999).

[12] Fiederling, R. *et al.* Injection and detection of a spin-polarized current in a light-emitting diode. *Nature* **402**, 787 (1999).

[13] Jonker, B. T. *et al.* Electrical spin-injection into silicon from a ferromagnetic metal/tunnel barrier contact. *Nature Phys.* **3**, 542 (2007).

[14] Lou, X. *et al.* Electrical detection of spin accumulation at a ferromagnet-semiconductor interface. *Phys. Rev. Lett.* **96**, 176603 (2006).

[15] Dash, S. P. *et al.* Electrical creation of spin polarization in silicon at room temperature. *Nature* **462**, 491–494 (2009).